



## Research paper

# Dysregulation of the splicing machinery is directly associated to aggressiveness of prostate cancer



Juan M. Jiménez-Vacas<sup>a,b,c,d</sup>, Vicente Herrero-Aguayo<sup>a,b,c,d</sup>, Antonio J. Montero-Hidalgo<sup>a,b,c,d</sup>, Enrique Gómez-Gómez<sup>a,b,c,e</sup>, Antonio C. Fuentes-Fayos<sup>a,b,c,d</sup>, Antonio J. León-González<sup>a,b,c,d</sup>, Prudencio Sáez-Martínez<sup>a,b,c,d</sup>, Emilia Alors-Pérez<sup>a,b,c,d</sup>, Sergio Pedraza-Arévalo<sup>a,b,c,d</sup>, Teresa González-Serrano<sup>a,c,f</sup>, Oscar Reyes<sup>a,c,g</sup>, Ana Martínez-López<sup>a,c,f</sup>, Rafael Sánchez-Sánchez<sup>a,c,f</sup>, Sebastián Ventura<sup>a,c,g</sup>, Elena M. Yubero-Serrano<sup>a,b,c,d,h</sup>, María J. Requena-Tapia<sup>a,c,e</sup>, Justo P. Castaño<sup>a,b,c,d</sup>, Manuel D. Gahete<sup>a,b,c,d</sup>, Raúl M. Luque<sup>a,b,c,d,\*</sup>

<sup>a</sup> Maimonides Institute for Biomedical Research of Córdoba (IMIBIC), Córdoba, Spain

<sup>b</sup> Department of Cell Biology, Physiology, and Immunology, University of Córdoba, Córdoba, Spain

<sup>c</sup> Hospital Universitario Reina Sofía (HURS), Córdoba, Spain

<sup>d</sup> Centro de Investigación Biomédica en Red de Fisiopatología de la Obesidad y Nutrición, (CIBERObn), Córdoba, Spain

<sup>e</sup> Urology Service, HURS/IMIBIC, Córdoba, Spain

<sup>f</sup> Anatomical Pathology Service, HURS, Córdoba, Spain

<sup>g</sup> Department of Computer Sciences, University of Córdoba, Córdoba, Spain

<sup>h</sup> Lipids and Atherosclerosis Unit, Reina Sofía University Hospital, Córdoba, Spain

## ARTICLE INFO

## Article History:

Received 24 July 2019

Revised 28 October 2019

Accepted 7 November 2019

Available online 3 January 2020

## Keywords:

Prostate cancer

Splicing

Spliceosome

SNRNP200

SRSF3

SRRM1

Therapeutic target

## ABSTRACT

**Background:** Dysregulation of splicing variants (SVs) expression has recently emerged as a novel cancer hallmark. Although the generation of aberrant SVs (e.g. AR-v7/sst5TMD4/etc.) is associated to prostate-cancer (PCa) aggressiveness and/or castration-resistant PCa (CRPC) development, whether the molecular reason behind such phenomena might be linked to a dysregulation of the cellular machinery responsible for the splicing process [spliceosome-components (SCs) and splicing-factors (SFs)] has not been yet explored.

**Methods:** Expression levels of 43 key SCs and SFs were measured in two cohorts of PCa-samples: 1) Clinically-localized formalin-fixed paraffin-embedded PCa-samples ( $n = 84$ ), and 2) highly-aggressive freshly-obtained PCa-samples ( $n = 42$ ).

**Findings:** A profound dysregulation in the expression of multiple components of the splicing machinery (i.e. 7 SCs/19 SFs) were found in PCa compared to their non-tumor adjacent-regions. Notably, overexpression of *SNRNP200*, *SRSF3* and *SRRM1* (mRNA and/or protein) were associated with relevant clinical (e.g. Gleason score, T-Stage, metastasis, biochemical recurrence, etc.) and molecular (e.g. AR-v7 expression) parameters of aggressiveness in PCa-samples. Functional (cell-proliferation/migration) and mechanistic [gene-expression (qPCR) and protein-levels (western-blot)] assays were performed in normal prostate cells (PNT2) and PCa-cells (LNCaP/22Rv1/PC-3/DU145 cell-lines) in response to *SNRNP200*, *SRSF3* and/or *SRRM1* silencing (using specific siRNAs) revealed an overall decrease in proliferation/migration-rate in PCa-cells through the modulation of key oncogenic SVs expression levels (e.g. AR-v7/*PKM2/XBP1s*) and alteration of oncogenic signaling pathways (e.g. p-AKT/p-JNK).

**Interpretation:** These results demonstrate that the spliceosome is drastically altered in PCa wherein *SNRNP200*, *SRSF3* and *SRRM1* could represent attractive novel diagnostic/prognostic and therapeutic targets for PCa and CRPC.

© 2019 The Author(s). Published by Elsevier B.V. This is an open access article under the CC BY-NC-ND license.

(<http://creativecommons.org/licenses/by-nc-nd/4.0/>)

## 1. Introduction

Dysregulation of the alternative splicing process is considered a key hallmark of cancer and could represent a novel source for the

identification of diagnostic, prognostic and therapeutic targets in highly prevalent tumor pathologies [1]. Specifically, alternative splicing represents an essential biological process by which the introns of an immature pre-mRNA are excised, and the exons are fused to generate mature mRNAs capable to be translated into functional proteins [2]. Indeed, most eukaryotic genes undergo alternative splicing, leading to a higher molecular flexibility through the increase of

\* Correspondence author.

E-mail addresses: [raul.luque@uco.es](mailto:raul.luque@uco.es), [bc2luhur@uco.es](mailto:bc2luhur@uco.es) (R.M. Luque).

## Research in context

### Evidence before this study

Early studies have demonstrated that the dysregulation of the expression of several splicing variants [e.g. Androgen receptor variant-7 (AR-v7), truncated somatostatin receptor SST<sub>5</sub>TMD4, In1-ghrelin, etc.] increases prostate cancer (PCa) aggressiveness and/or promotes resistance to the available drugs currently used in clinical practice (e.g. antiandrogens), hampering the treatment and the management of PCa patients. In this context, it is well known that this process is catalyzed by a macromolecular machinery (i.e. spliceosome) and regulated by specific proteins (i.e. splicing factors; SFs). However, the putative dysregulation of spliceosome components (SCs) and splicing factors in PCa as well as the potential of these elements as diagnostic, prognostic and/or therapeutic tools for this pathology remain poorly known.

### Added value of this study

Our study demonstrates that the expression of several SCs and SFs are drastically dysregulated in PCa tissues compared with control (non-tumoral) tissues. Of particular importance is the demonstration that the changes in the expression of SNRNP200, SRSF3 and SRRM1 (at the mRNA and protein level) are associated to key clinical features of aggressiveness (e.g. Gleason score, biochemical recurrence, presence of metastasis, vascular and perineural invasion) in PCa patients as well as to important molecular phenotypes (e.g. AR-v7 expression) of PCa. Notably, this study also shows that the silencing of the expression of SNRNP200, SRRM1 and SRSF3: 1) evoked clear antitumor actions in PCa cells (e.g. inhibition of proliferation, migration) through the modulation of key oncogenic signaling pathways (e.g. PI3K/AKT, ERK, JNK) and splicing variants (e.g. AR-v7, PKM2, XBP1s), and, 2) was able to re-sensitize PCa cells to enzalutamide treatment, pointing out the potential therapeutic utility of these elements for the most aggressive phenotype of PCa, castration resistant PCa, which remains lethal nowadays.

### Implications of all the available evidence

Altered expression of splicing machinery elements (spliceosome components and splicing factors) might be associated with the development, progression and aggressiveness of PCa. Our data demonstrate the existence of a splicing machinery-associated molecular dysregulation that could be potentially considered as a source of novel diagnostic and prognostic biomarkers as well as therapeutic targets for PCa. Specifically, our results reveal that three components of the splicing machinery (SNRNP200, SRSF3 and SRRM1) could represent potential, global and effective therapeutic targets to tackle this devastating pathology.

homeostasis and, therefore, the dysregulation of this process has been associated to different diseases, including endocrine-metabolic and tumor pathologies [2].

In this scenario, it has been shown that alternative splicing contributes to the heterogeneity, aggressiveness and resistance to medical treatment of prostate cancer (PCa), one of the most important public health problems worldwide with numbers of cases increasing significantly every year [3]. In this context, several studies have demonstrated that the androgen receptor (AR) gene is a source of splicing variants (SVs), especially AR-v7, which is a key driver for PCa progression (e.g. increased risk of biochemical relapse and inferior overall survival outcomes). In addition, a number of cancer-specific SVs has been identified in PCa, including SST<sub>5</sub>TMD4 [4], PKM2 [5], REST4 [6], XBP1s [7], In1-Ghrelin [8] etc., which also play an oncogenic role in this tumor pathology. In fact, it has been proposed that the “splicing signature” represents a more accurate parameter to stratify patients than the “transcriptome signature”, which is typically analysed by conventional microarray analyses [9]. Thus, the understanding of the regulation of splicing in normal and pathological prostate cells may help to identify novel biomarkers and therapeutic targets for this devastating tumor pathology. However, to the best of our knowledge, to date no studies have been focused on the mechanisms driving the generation of the SVs (i.e. the regulation of the splicing machinery), which might provide new contexts for the development of novel strategies to tackle PCa, since targeting the activity of selected spliceosome components that may be dysregulated in PCa could serve to inhibit the generation of oncogenic SVs (e.g. AR-v7), representing an attractive therapeutic strategy for PCa. Therefore, in this study we aimed to determine for the first time the expression levels of a representative set of spliceosome components (SCs) and SFs and their relationship with clinical and molecular features of PCa-aggressiveness, as well as its pathological role in this disease.

## 2. Material and methods

### 2.1. Patients and samples

This study was approved by the Reina Sofia University Hospital Ethics Committee and was conducted in accordance with the principles of the Declaration of Helsinki. The regional Biobank coordinated the collection, processing, management and assignment of the biological samples used in the present study according to the standard procedures established for this purpose. Written informed consent was obtained from all patients. Two different cohorts of prostate samples were included in this study:

- **Cohort 1** formalin-fixed, paraffin-embedded (FFPE) PCa tissues ( $n=84$ ) and their non-tumor adjacent region (N-TAR; used as control tissues;  $n=84$ ), taken from radical prostatectomies from patients diagnosed with clinically localized PCa (Table 1).
- **Cohort 2** fresh PCa samples ( $n=42$ ) that were obtained by core needle biopsies from patients with suspect of presenting significant PCa [defined as Gleason score (GS)  $\geq 7$ ; highly aggressive PCa], which was further confirmed histologically by uro-pathologists (Table 2).

The clinical parameters collected from each patient were GS (analysed by uro-pathologists following the modified 2005, 2010 and 2014 ISUP criteria, based on the sample collection date), T-Stage, perineural invasion, lymphovascular invasion, presence of metastases at diagnosis (determined by computed tomography and bone scan) and biochemical recurrence (defined by two consecutive PSA values  $> 0.2$  ng/mL and rising, after radical prostatectomy).

transcripts generated from a given gene [2]. Unfortunately, dysregulations of this process are associated to the appearance of diverse protein isoforms that could exhibit strong pathological potential [1]. In eukaryotes, the control of the appropriate splicing process is orchestrated by the spliceosome, a complex cellular machinery comprised by different small nuclear ribonucleoproteins (RNU1, RNU2, etc.) and core spliceosome-associated proteins (PRPF8, PRPF40A, U2AF2, SF3B1, etc.). The spliceosome dynamically interacts with additional proteins (splicing factors; SFs) to finely recognize the introns and exons to be processed and to catalyze the splicing process of the pre-RNAs [1]. The appropriate functioning of this cellular machinery is essential to maintain the cellular, tissue and body

**Table 1**

Demographic, biochemical and clinical parameters of the patients with clinically localized PCa (Cohort 1). PSA: Prostate specific antigen; SigPCa: Significant PCa, defined as Gleason score  $\geq 7$ ; pT: Pathological primary tumor staging; PI: Perineural invasion; VI: Vascular invasion.

Parameter	
Patients [n]	84
Age, years [median (IQR)]	61 (57–66)
PSA levels, ng/mL [median (IQR)]	5.2 (4.2–8.0)
Sig PCa [n (%)]	76 (90.5%)
pT $\geq 3a$ [n (%)]	59 (70.2%)
PI [n (%)]	72 (85.7%)
VI [n (%)]	8 (9.52%)
Recurrence [n (%)]	35 (41.7%)
Metastasis [n (%)]	0 (0%)

## 2.2. Cell cultures

PCa cell lines (LNCaP, 22Rv1, PC-3 and DU145) were obtained from American Type Culture Collection (ATCC; Manassas, VA, USA) while normal prostate cell line PNT2 was a kind gift from Dr. J. De Bono. These cell lines were cultured according to manufacturer instructions as previously described [4,8,10], validated by analysis of short tandem repeats (STRs) sequences using GenePrint 10 System (Promega, Barcelona, Spain) and checked for mycoplasma contamination by PCR as previously reported [4]. For functional assays, LNCaP, 22Rv1 and DU145 cell lines were used. For mechanistic assays, 22Rv1 cells were used since this cell line represents a PCa model with AR and AR-v7 expression.

## 2.3. Transfection with specific siRNAs

For silencing assays, LNCaP, 22Rv1 and DU145 cell lines were used. Specifically, 200,000 cells were seeded in 6-well plates and grown until 70% of confluence was reached. Then, cells were transfected with specific siRNAs against *SNRNP200* (#124735; Thermo Fisher Scientific, Madrid, Spain), *SRRM1* (s20018; Thermo Fisher Scientific) and *SRSF3* (s12733; Thermo Fisher Scientific) at 100 nM, using Lipofectamine-RNAiMAX (Thermo Fisher Scientific) as previously reported [22]. After 24h, cells were collected for quantitative-PCR (qPCR), western blot, cell proliferation and/or cell migration assays.

## 2.4. Cell proliferation

In order to determine the effect of the silencing of *SNRNP200*, *SRRM1* and *SRSF3* on cell proliferation, Alamar-Blue assay (Bio-Source International, Camarillo, CA, USA) was performed in LNCaP, 22Rv1 and DU145 cell lines, as previously reported [4]. Briefly, cells were seeded in 96-well plates at a density of 3,000–5,000 cells/well and serum-starved for 24h, then cell proliferation was evaluated using the FlexStation III system (Molecular Devices, Sunnyvale, CA, USA) until 72 h.

**Table 2**

Demographic, biochemical and clinical parameters of the patients with highly aggressive PCa (Cohort 2). PSA: Prostate specific antigen; SigPCa: Significant PCa defined as Gleason score  $\geq 7$ .

Parameter	
Patients [n]	42
Age, years [median (IQR)]	75 (69–81)
PSA levels, ng/mL [median (IQR)]	62.0 (36.2–254.5)
SigPCa [n (%)]	42 (100%)
Metastasis [n (%)]	28 (66.7%)

## 2.5. Enzalutamide-sensitization assay

To test the role of *SNRNP200*, *SRRM1* and *SRSF3* on the response to enzalutamide treatment (#1613, Axon Medchem, Groningen, The Netherlands), cell proliferation was evaluated. Specifically, LNCaP and 22Rv1 cells were acclimated during 24h to RPMI 1640 without phenol-red supplemented with charcoal-stripped serum (#A3382101; Thermo Fisher Scientific). Then, scrambled- or siRNA-transfected cells were treated with enzalutamide at 1  $\mu$ M. All cells were treated with 5 $\alpha$ -dihydrotestosterone (DHT; # D-073; Merck, Madrid, Spain) at 10 nM. Cell proliferation was calculated, after 24h of treatment, as described above. Results were expressed as percentage referred to scramble treated with vehicle (DMSO) plus DHT treatment.

## 2.6. Cell migration

Cell migration was evaluated by wound-healing assay in DU145 cell line in response to *SNRNP200*, *SRRM1*, *SRSF3* silencing, due to the inability of LNCaP and 22Rv1 cells to migrate. Specifically, images of the scratch were taken at 0 and 12 h and wound healing was calculated as the area observed 12 h after the wound was made vs. the area observed just after wounding, as previously described [4]. Results were expressed as percentage referred to scramble.

## 2.7. Western blot

Protein levels of several PCa-related genes were analysed in 22Rv1 cells as previously reported [4]. Briefly, 200,000 cells were seeded in 12-well plates and after two days, proteins were extracted using pre-warmed (65 °C) SDS-DTT buffer (62.5 mM Tris-HCl, 2% SDS, 20% glycerol, 100 mM DTT, and 0.005% bromophenol blue). Then, proteins were sonicated for 10 s and boiled for 5 min at 95 °C. Proteins were separated by SDS-PAGE and transferred to nitrocellulose membranes (Millipore, Billerica, MA, USA). Membranes were blocked with 5% non-fat dry milk in Tris-buffered saline/0.05% Tween 20 and incubated overnight with the specific antibodies for phospho-AKT (#4060S; Cell Signaling, Leiden, NLD), phospho-ERK (#4370S; Cell Signaling), phospho-JNK (AF1205; R&D-Systems, Minneapolis, MN, USA), AKT (#9272S; Cell Signaling), ERK (sc-154; Santa Cruz Biotechnology, Dallas, TX, USA), JNK (AF1387; R&D Systems), *SNRNP200* (ab241589; Abcam, Camdridge, UK), *SRRM1* (PA5-69086; Thermo Fisher Scientific), *SRSF3* (ab198291; Abcam) and the secondary antibody HRP-conjugated goat anti-rabbit IgG (#7074 s; Cell Signaling). Specifically, the specificity of *SNRNP200* and *SRSF3* antibodies was validated in our laboratory by western blot and ICC (only 1 band was recognized by western blot and depletion of protein quantity was observed in response to specific siRNAs using western blot and ICC approaches). *SRRM1* specificity was not completely validated since more than 1 band was recognized in western blot (however, depletion of protein quantity was observed in response to a specific siRNAs using western blot and ICC approaches). Proteins were detected using an enhanced chemiluminescence detection system (GEHealthcare, Madrid, Spain) with dyed molecular weight markers (Bio-Rad, Madrid, Spain). A densitometry analysis of the bands obtained was carried out with ImageJ software, using total AKT, ERK and JNK protein levels as normalizing factor for phospho-AKT, phospho-ERK and phospho-JNK, respectively.

## 2.8. RNA extraction

Total RNA from FFPE samples was isolated and DNase-treated using the Maxwell 16 LEVRNA FFPE Kit (Promega, Madison, WI, USA) according to manufacturer instructions in the Maxwell MDx 16 Instrument (Promega, Madrid, Spain). Additionally, total RNA was extracted from fresh samples using the AllPrep DNA/RNA/Protein

Mini Kit (Qiagen) and from PCa cell lines using TRIzol Reagent (Thermo Fisher Scientific, Waltham, MA, USA), followed, in both cases, by DNase treatment using RNase-Free DNase Kit (Qiagen, Hilden, DEU). Total RNA concentration and purity was assessed using Nanodrop One Spectrophotometer (Thermo Fisher Scientific). Total RNA was retrotranscribed using random hexamer primers and the cDNA First Strand Synthesis kit (Thermo Fisher Scientific).

### 2.9. qPCR dynamic array based on microfluidic technology

A qPCR dynamic array based on microfluidic technology that allows the determination of the expression of 45 transcripts in 48 samples, simultaneously, (Fluidigm, San Francisco, CA, USA) was implemented. Specific primers for human transcripts including components of the major spliceosome ( $n = 10$ ), minor spliceosome ( $n = 4$ ), associated SFs ( $n = 25$ ) and three housekeeping genes (*ACTB*, *GAPDH* and *HPRT*) were specifically designed with the Primer3 software and StepOne™ Real-Time PCR System software v2.3 (Applied Biosystems, Foster City, CA, USA) (Supplemental Table 1). Preamplification, exonuclease treatment and qPCR dynamic array based on microfluidic technology were implemented as recently reported [11,12], following manufacturer's instructions using the Biomark System and the Real-Time PCR Analysis Software (Fluidigm). To control for variations in the efficiency of the retro-transcription reaction, mRNA copy numbers of the different transcripts analysed were adjusted by normalization factor, calculated with the expression levels of *ACTB* and *GAPDH* using GeNorm 3.3 [13].

### 2.10. RNA retrotranscription and quantitative real-time PCR

Details regarding the development, validation, and application of the quantitative real-time PCR to measure expression levels of the transcripts of interest have been previously reported by our laboratory [14–17]. Specific primers set used to measure the expression levels of the genes of interest in this study are described in Supplemental Table 2. Specifically, primers for *KLF6-SV1*, *KLF6*, *PKM2*, *PKM1*, *REST4* and *REST* transcripts were obtained from previous studies [18–20]. To control for variations in the efficiency of the retro-transcription reaction, mRNA copy numbers of the different transcripts analysed were adjusted by a normalization factor which was calculated with the expression levels of *ACTB* and *GAPDH* using GeNorm 3.3 [13].

### 2.11. Immunohistochemistry (IHC) analysis

IHC analysis was performed on FFPE prostate samples that were obtained by core needle biopsies from patients of cohort 2, since they represent the most aggressive cohort of our study ( $GS \geq 7$ ). Samples of benign prostatic hyperplasia (BPH), prostatic intraepithelial neoplasia (PIN) and non-significant PCa with  $GS = 6$  ( $n = 7, 6$  and  $5$ , respectively) also taken by core needle biopsies were included in this analysis as control samples and low aggressive PCa, respectively. Briefly, deparaffinized sections were incubated overnight ( $4^\circ\text{C}$ ) with the primary antibodies against the proteins of interest [i.e. *SNRNP200* (ab241589; Abcam), *SRRM1* (PA5-69086; Thermo Fisher Scientific) or *SRSF3* (ab198291; Abcam)] at 1:250 dilution, followed by incubation with an anti-rabbit horseradish peroxidase-conjugated secondary antibody (#7074; Cell Signaling). Finally, sections were developed with 3,3'-diaminobenzidine (Envision system 2-Kit Solution DAB) and contrasted with haematoxylin. Two independent pathologists performed histopathologic analyses indicating low, moderate, and high intensities of staining, following a blinded protocol.

### 2.12. Statistical and bioinformatic analyses

Statistical differences between two groups were calculated by unpaired parametric *t*-test or nonparametric Mann Whitney U test, according to normality, assessed by Kolmogorov-Smirnov test. For differences among three groups, One-Way ANOVA analysis was performed. Spearman's or Pearson's bivariate correlations were performed for quantitative variables according to normality. Significant relation between categorized mRNA expression and biochemical PCA recurrence was studied using the long-rank-p-value method. Predictive models were constructed by Random Forest algorithm (with R language) as classifier as previously reported [11,12]. The rest of the statistical analyses were assessed using GraphPad Prism 7 (GraphPad Software, La Jolla, CA) or SPSS version 17.0. All the experiments were performed in, at least, 3 independent times ( $n \geq 3$ ), and with at least 2 technical replicates. Statistical significance was considered when  $p < 0.05$ . A trend for significance was indicated when p-values ranged between  $> 0.05$  and  $< 0.1$ .

## 3. Results

### 3.1. Expression levels of spliceosome components and splicing factors are dysregulated in PCa and are associated with clinical and molecular aggressiveness features

The expression levels of 26 out of 45 (58%) genes involved in the pre-RNA splicing process were found to be significantly dysregulated in PCa-tissues compared to their respective control-tissues (N-TAR) from a cohort of patients with clinically-localized PCa ( $n = 84$ ; Table 1; Fig. 1a/b). Specifically, the SCs *RNU4*, *RNU6*, *PRPF40A*, *SF3B1*, *SNRNP200*, *U2AF2* and *RNU12* were overexpressed in PCa-tissues (Fig. 1a). Additionally, the SFs *ESRP1*, *ESRP2*, *KHDRBS1*, *MAGOH*, *NOVA1*, *PTBP1*, *RBM3*, *RBM45*, *SND1*, *SRSF2*, *SRSF3*, *SRSF4*, *SRSF5*, *SRSF9*, *SRSF10*, *SRRM1*, *TIA1* and *TRA2A* were also overexpressed while the SF *SRRM4* was down-regulated in PCa-tissues (Fig. 1b). No statistically significant differences were observed in the expression levels of the rest of SCs and SFs analysed (Supplemental Figure 1). Non-supervised clustering bioinformatic approaches (Random Forest algorithm) revealed that the molecular fingerprint comprised by the combination of the expression of *SNRNP200*, *SRRM1*, *SRSF3*, *TIA1*, *SRSF10*, *U2AF2*, *SRSF9*, *SRRM4*, *SND1*, *ESRP1*, and *KHDRBS1* perfectly discriminated between PCa and N-TARs samples with an AUC=1 (Fig. 1c). This was further supported by cross-validation analysis of this molecular fingerprint (AUC=0.83,  $p < 0.0001$ ; Fig. 1d).

Notably, the expression levels of the 85% (22 out of 26) SCs and SFs found dysregulated herein were significantly associated and/or correlated with at least one clinical parameter of PCa-aggressiveness (Tables 3 and 4). Remarkably, *SNRNP200*, *SRRM1* and *SRSF3* were the only genes whose expression was directly associated/correlated with all the clinical parameters of aggressiveness (Gleason score, T-Stage, perineural- and lymphovascular-invasion; Table 3; Fig. 1e) and progression (biochemical recurrence; Table 4; Fig. 1f) available in this cohort of patients. In addition, *in silico* data showed the overexpression in PCa samples of *SNRNP200* in Singh, Wallace and Welsh datasets. Moreover, *SRRM1* was found to be overexpressed in PCa samples in Welsh and Tomlins datasets, while a trend was observed in Wallace dataset ( $p = 0.089$ ). On the other hand, an overexpression of *SRSF3* in PCa samples was found in Singh and Tomlins datasets (Supplemental Figure 2).

Based on these results, we further analysed the expression levels of *SNRNP200*, *SRRM1* and *SRSF3* in an independent and more aggressive cohort of PCa-samples (Table 2). These analyses revealed an association between the elevated expression levels of *SNRNP200*, *SRRM1* and *SRSF3* in PCa-samples and the presence of metastases at the moment of diagnosis (Fig. 2a). *SNRNP200* and *SRSF3* expression tended to be positively correlated with Gleason score ( $p = 0.053$ ,

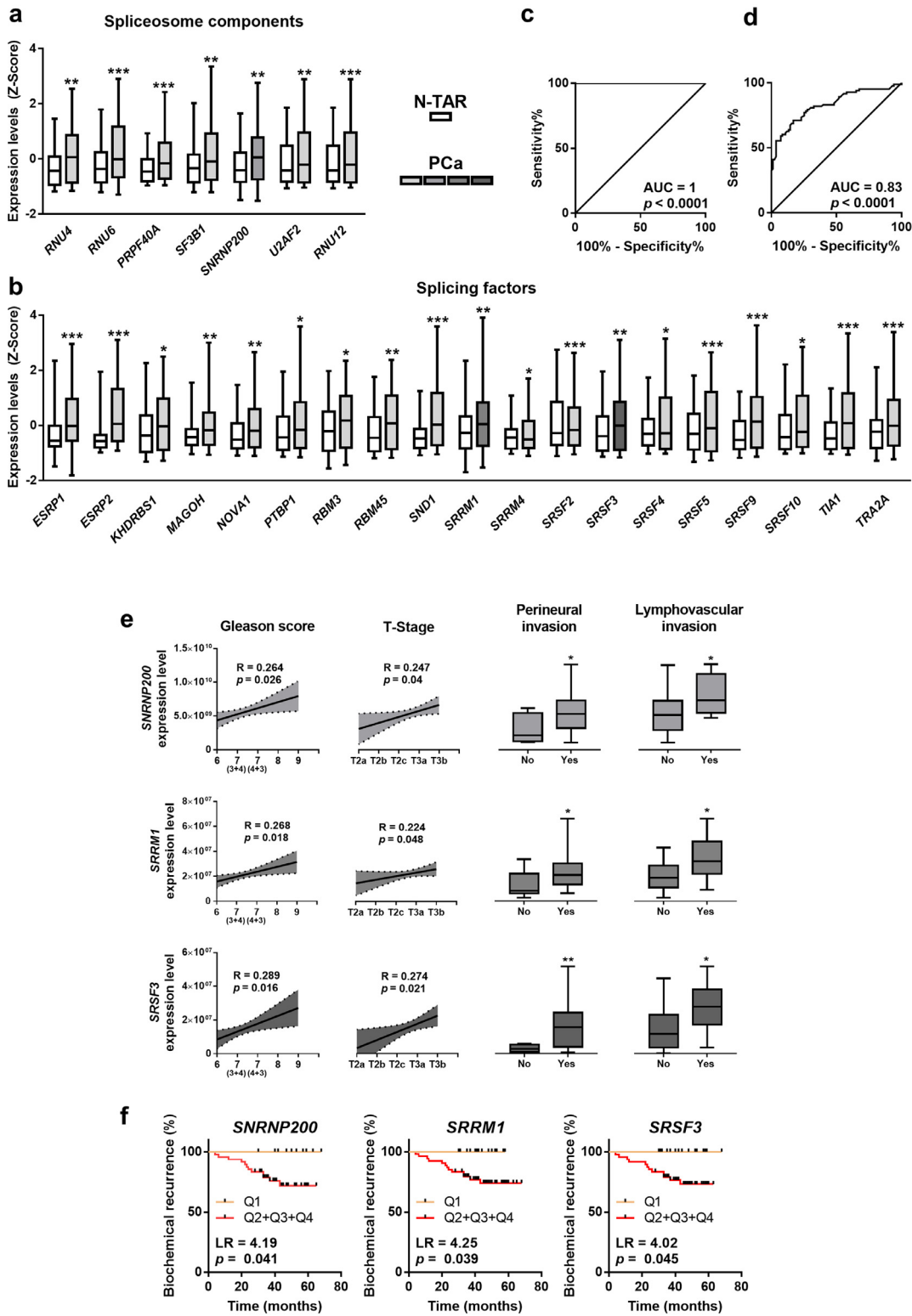


**Fig. 1.** Expression of spliceosome components and splicing factors in prostate cancer (PCa) samples. (a–b) Comparison of mRNA levels of spliceosome components (a) and splicing factors (b) between formalin-fixed paraffin embedded (FFPE) samples from PCa samples and non-tumor adjacent regions (N-TAR) ( $n = 84$ ) determined by a microfluidic-based qPCR array. Data represent the mean  $\pm$  SEM of mRNA expression levels adjusted by normalization factor (calculated from *ACTB* and *GAPDH* expression levels) and standardized by Z-score. c-d) ROC curves of a subset of spliceosome components and splicing factors generated by Random Forest computational algorithm (c) followed by cross validation analysis (d) to distinguish between tumor and N-TAR samples. e) Association between the expression levels of selected spliceosome components and splicing factors (*SNRNP200*, *SRRM1* and *SRSF3*) and clinical parameters (Gleason score, T-Stage, perineural and lymphovascular invasion) in the same cohort of FFPE samples ( $n = 84$ ). Correlations are represented by mean (connecting line) and error bands (pointed line) of expression levels. Data of associations represent the mean  $\pm$  SEM of mRNA expression levels adjusted by normalization factor (calculated from *ACTB* and *GAPDH* expression levels). f) Association between *SNRNP200*, *SRRM1* and *SRSF3* expression levels and biochemical PCa recurrence in 67 samples from FFPE cohort (samples from patients who underwent adjuvant radiotherapy were not included), calculated by Log Rank analysis (LR). mRNA levels were determined by a microfluidic-based qPCR array and adjusted by normalization factor calculated from *ACTB* and *GAPDH* expression levels. Asterisks (\*  $p < 0.05$ ; \*\*  $p < 0.01$ ; \*\*\*  $p < 0.001$ ) indicate statistically significant differences between groups.

**Table 3**

Correlation and association of *SNRNP200*, *SRRM1* and *SRSF3* expression levels with clinical features of prostate cancer aggressiveness. Data of correlations represent the coefficient "r". Data of associations represent the difference between means of each group  $\pm$  standard deviation. Significant prostate cancer (SigPca) is defined as Gleason score  $\geq$  7. Asterisks (\*  $p < 0.05$ ; \*\*  $p < 0.01$ ; \*\*\*  $p < 0.001$ ) indicate statistically significant differences between groups.

	Correlations		Associations		
	Gleason score	T- Stage	Perineural Invasion	Lymphovascular Invasion	SigPca
<i>RNU4</i>	0.122	<b>0.239*</b>	<b>9,664,718,823 <math>\pm</math> 3,162,530,673 **</b>	<b>7,730,140,948 <math>\pm</math> 3,078,119,236 *</b>	<b>7,526,218,231 <math>\pm</math> 3,298,861,131 *</b>
<i>RNU6</i>	<b>0.235*</b>	0.075	<b>230,034,826 <math>\pm</math> 72,616,606 **</b>	119,362,920 $\pm$ 102,513,311	<b>163,738,961 <math>\pm</math> 75,084,561 *</b>
<i>PRPF40A</i>	0.184	0.214	<b>1,801,231 <math>\pm</math> 878,336 *</b>	1,669,010 $\pm$ 855,998	<b>1,789,300 <math>\pm</math> 832,618 *</b>
<i>SF3B1</i>	<b>0.312**</b>	0.121	<b>9,003,875 <math>\pm</math> 3,487,752 *</b>	<b>10,853,954 <math>\pm</math> 4,783,529 **</b>	5,808,930 $\pm$ 3,941,225
<i>U2AF2</i>	0.09	0.083	<b>714,287 <math>\pm</math> 348,778 *</b>	807,889 $\pm$ 481,128	347,329 $\pm$ 370,880
<i>SNRNP200</i>	<b>0.264*</b>	<b>0.247*</b>	<b>2,681,185,105 <math>\pm</math> 1,175,955,224 *</b>	<b>2,812,777,484 <math>\pm</math> 1,275,566,115 *</b>	<b>2,125,357,393 <math>\pm</math> 1,042,911,480 *</b>
<i>RNU12</i>	<b>0.321**</b>	0.178	<b>395,441 <math>\pm</math> 132,486 **</b>	133,816 $\pm$ 149,579	208,236 $\pm$ 139,628
<i>ESRP1</i>	<b>0.319**</b>	0.166	1,658,118 $\pm$ 916,550	2,151,271 $\pm$ 1,084,569	<b>1,874,015 <math>\pm</math> 936,328 *</b>
<i>ESRP2</i>	<b>0.281*</b>	<b>0.254*</b>	1,953,298 $\pm$ 1,179,570	<b>3,964,985 <math>\pm</math> 1,266,549 **</b>	<b>2,941,102 <math>\pm</math> 1,300,974 *</b>
<i>KHDRBS1</i>	0.128	0.215	<b>8,816,079 <math>\pm</math> 4,355,945 *</b>	7,047,264 $\pm$ 5,942,380	<b>10,326,770 <math>\pm</math> 4,988,242 *</b>
<i>MAGOH</i>	<b>0.331**</b>	0.173	572,836 $\pm$ 376,052	<b>1,036,475 <math>\pm</math> 489,737 *</b>	772,768 $\pm$ 395,132
<i>NOVA1</i>	0.131	0.211	1,375,554 $\pm$ 1,240,422	<b>2,891,594 <math>\pm</math> 1,397,232 *</b>	1,968,158 $\pm$ 1,417,671
<i>PTB</i>	0.189	0.197	462,842 $\pm$ 504,081	707,443 $\pm$ 685,520	923,496 $\pm$ 547,502
<i>RBM3</i>	0.141	0.139	1,831,860 $\pm$ 1,133,513	<b>2,948,642 <math>\pm</math> 1,333,148 *</b>	2,051,801 $\pm$ 1,189,264
<i>RBM45</i>	0.145	0.159	2,144,099 $\pm$ 1,086,705	2,444,946 $\pm$ 1,430,495	1,613,514 $\pm$ 1,237,865
<i>SND1</i>	<b>0.236*</b>	0.167	<b>6,829,797 <math>\pm</math> 3,127,408 *</b>	<b>8,116,316 <math>\pm</math> 3,698,131 *</b>	<b>7,483,290 <math>\pm</math> 3,461,207 *</b>
<i>SRSF2</i>	<b>0.284*</b>	0.161	<b>903,780 <math>\pm</math> 409,990 *</b>	<b>1,099,682 <math>\pm</math> 533,886 *</b>	914,182 $\pm$ 460,892
<i>SRSF3</i>	<b>0.289*</b>	<b>0.274*</b>	<b>13,698,858 <math>\pm</math> 5,050,576 **</b>	<b>12,653,631 <math>\pm</math> 5,712,504 *</b>	<b>10,070,038 <math>\pm</math> 5,031,330 *</b>
<i>SRSF4</i>	0.139	0.169	<b>2,131,612 <math>\pm</math> 857,251 *</b>	<b>3,422,072 <math>\pm</math> 1,068,338 **</b>	941,268 $\pm$ 902,489
<i>SRSF5</i>	0.055	0.129	<b>105,348,741 <math>\pm</math> 37,924,790 **</b>	<b>141,185,003 <math>\pm</math> 48,026,387 **</b>	35,477,260 $\pm$ 37,643,655
<i>SRSF9</i>	0.088	0.211	<b>33,397,890 <math>\pm</math> 12,917,648 *</b>	28,501,453 $\pm$ 15,538,733	26,539,564 $\pm$ 14,468,693
<i>SRSF10</i>	0.057	0.218	<b>10,135,257 <math>\pm</math> 4,077,596 *</b>	10,622,878 $\pm$ 5,604,567	4,248,356 $\pm$ 4,293,783
<i>SRRM1</i>	<b>0.211*</b>	<b>0.224*</b>	<b>9,522,292 <math>\pm</math> 4,314,271 *</b>	<b>9,444,197 <math>\pm</math> 4,007,860 *</b>	<b>9,478,531 <math>\pm</math> 4,760,093 *</b>
<i>SRRM4</i>	-0.154	0.107	53,981 $\pm$ 33,971	-2375 $\pm$ 34,689	47,458 $\pm$ 36,610
<i>TIA1</i>	0.114	<b>0.246*</b>	<b>5,965,156 <math>\pm</math> 2,459,924 *</b>	6,334,929 $\pm$ 2,989,097	<b>5,493,989 <math>\pm</math> 2,630,409 *</b>
<i>TRA2A</i>	0.141	0.191	<b>27,361,791 <math>\pm</math> 12,693,441 *</b>	39,100,412 $\pm$ 15,368,002	29,010,940 $\pm$ 15,801,444

$R = 0.308$ ;  $p = 0.086$ ,  $R = 0.290$ ; respectively; Fig. 2b). Furthermore, *SNRNP200*, *SRRM1* and/or *SRSF3* expression directly correlated with the expression levels of the oncogenic SV *AR-v7* [(Fig. 2c); but not with *AR* expression (Fig. 2d)], with *MKI67* (Fig. 2e) and *KLK3* (i.e. *SRSF3* and *SRRM1*, but not *SNRNP200*; Fig. 2f).

### 3.2. Protein levels of *SNRNP200*, *SRRM1* and *SRSF3* are elevated in PCa samples and associated with clinical aggressiveness features

IHC analyses using FFPE samples from the cohort of patients with highly-aggressive PCa (Table 2) revealed that *SNRNP200*, *SRSF3* and *SRRM1* protein levels were significantly higher in PCa-samples compared to controls samples (FFPE samples of patients with PIN and/or BPH). Specifically, nuclear staining of *SNRNP200* was higher in PCa samples compared to PIN and BPH samples. Low levels of cytoplasmic *SNRNP200* protein were detected, while no changes were observed among groups (data not shown). Furthermore, although cytoplasmic protein level of *SRRM1* was not detected, *SRRM1*-nuclear levels were significantly higher in PCa-samples compared to BPH and PIN samples (Fig. 3b). In contrast, no differences among *SRSF3*-nuclear staining were found between PCa, BPH and PIN samples (data not shown); however, *SRSF3*-cytoplasmic staining was significantly higher in PCa and PIN samples compared to BPH samples (Fig. 3c). Finally, *SNRNP200*, *SRRM1* and *SRSF3* protein levels were associated with clinically significant PCa (SigPCa; Gleason score  $\geq$  7) and, in the case of *SRRM1* and *SRSF3*, tended to be associated with the presence of metastasis ( $p = 0.077$ ,  $p = 0.067$ , respectively).

### 3.3. Silencing of *SNRNP200*, *SRRM1* and *SRSF3* expression decreases functional parameters of aggressiveness in PCa cells

The analysis of the expression levels of *SNRNP200*, *SRRM1* and *SRSF3* in prostate-derived cell lines showed that: 1) *SNRNP200* was

overexpressed in the PCa-derived cell lines 22Rv1, LNCaP and DU145 compared to the normal-like prostate cell line PNT2 (Fig. 4a, left-panel); 2) *SRRM1* was significantly overexpressed in all the PCa cell lines compared to PNT2 (Fig. 4a, middle-panel); and, 3) that *SRSF3* was overexpressed in 22Rv1, DU145 and PC-3 compared to PNT2 (Fig. 4a, right-panel). Therefore, we selected an androgen-dependent  $AR^+/AR-v7^-$  model (LNCaP), an androgen-independent  $AR^+/AR-v7^-$  model (22Rv1) and an androgen independent  $AR^-/AR-v7^-$  model (DU145) to perform functional experiments in response to the silencing of these three genes. The silencing of *SNRNP200*, *SRRM1* and *SRSF3* in response to specific siRNAs was validated at mRNA levels in LNCaP, 22Rv1 and DU145 cells (Fig. 4b), as well as at protein levels in DU145 cells (Supplemental Figure 3). Remarkably, no effects in proliferation rate were observed in response to scramble-siRNA in LNCaP, 22Rv1 and DU145 as compared to non-transfected cells (Supplemental Figure 4). Specifically, proliferation rate of LNCaP cells significantly decreased at 48 and 72 h in response to *SNRNP200*- and *SRRM1*-silencing, as well as at 24, 48 and 72 h in response to *SRSF3*-silencing (Fig. 4c) compared to scramble-transfected cells. Moreover, the silencing of *SNRNP200*, *SRRM1* and *SRSF3* significantly decreased proliferation rate (at 48 and 72 h) in 22Rv1 and DU145 (Fig. 4c). In addition, silencing of *SNRNP200*, *SRSF3*, but not *SRRM1*, reduced migration rate in DU145 cells (Fig. 4d).

### 3.4. Silencing of *SNRNP200*, *SRRM1* and *SRSF3* modulates relevant signaling pathways and the expression of oncogenic splicing variants in PCa

The silencing of *SRRM1* significantly decreased the phosphorylation levels of ERK, while silencing of *SRSF3* increased phosphorylation levels of ERK and decreased that of JNK (Fig. 5a). In contrast, no statistically significant changes in the phosphorylation levels of ERK, ERK or JNK were observed in response to *SNRNP200*-silencing (Fig. 5a).

**Table 4**  
Association of expression levels of spliceosome components and splicing factors with the development of biochemical recurrence of prostate cancer.

Factor	LongRank	p value
RNU4	1.822	0.177
RNU6	5.046	0.025
PRPF40A	4.938	0.026
SF3B1	4.012	0.045
U2AF2	4.222	0.040
RNU12	2.844	0.092
ESRP1	3.201	0.074
ESRP2	5.049	0.025
KHDRBS1	4.455	0.035
MAGOH	2.540	0.111
NOVA1	4.758	0.029
PTBP1	4.407	0.036
RBM3	1.631	0.202
RBM45	5.075	0.024
SND1	4.992	0.025
SRSF2	4.632	0.031
SRSF4	3.722	0.054
SRSF5	3.944	0.047
SRSF9	4.349	0.037
SRSF10	3.971	0.046
SRRM4	1.703	0.192
TIA1	4.551	0.033
TRA2A	4.702	0.030

The silencing of the expression of *SNRNP200*, *SRRM1* and *SRSF3* reduced the expression levels of the oncogenic splicing variants *PKM2*, *CASP2S* and *XBP1s*, without altering the expression of *PKM1*, *CASP2* and *XBP1u*. Therefore, *SNRNP200*-, *SRRM1*- and *SRSF3*-silencing decreased *PKM2/PKM1*, *CASP2S/CASP2* and *XBP1s/XBP1u* ratio (Fig. 5b). Moreover, only *SRRM1*-silencing resulted in a decrease in

the *REST4/REST* expression ratio (by a reduction of *REST4* without alteration of *REST*) and in a reduction of *KLF6-SV1* expression (Fig. 5b). In the case of *AR* splicing process, silencing of *SNRNP200* and *SRRM1* (but not *SRSF3*) evoked a decrease in the ratio of the *AR-v7/AR* expression, by a reduction of *AR-v7* without altering *AR* expression; while the silencing of *SRSF3* decreased both *AR-v7* and *AR* expression. Due to the importance of *AR-v7* on PCa aggressiveness, we determined whether *SNRNP200* and *SRRM1* could control the expression levels of splicing factors previously associated to the modulation of *AR* gene splicing and with *AR-v7* generation [i.e. *KHDRBS1* [21], *SFPQ* [22] and *U2AF2* [23]]. However, the expression levels of *KHDRBS1*, *SFPQ* and *U2AF2* were not significantly altered in response to the silencing of *SNRNP200* or *SRRM1* (Fig. 5c). In addition, no statistically significant changes were observed in the expression of additional splicing variants, such as *SST5TMD4* and *In1-ghrelin*, in response to *SNRNP200*-, *SRRM1*- and *SRSF3*-silencing (Fig. 5b).

Finally, expression levels of classical markers of PCa aggressiveness were analysed in response to *SNRNP200*-, *SRRM1*- and *SRSF3*-silencing. Specifically, *C-MYC* expression levels were reduced in response to *SRSF3*-silencing, while those of *TP53* were increased in response to *SNRNP200*-silencing (Fig. 5d). In addition, the silencing of *SNRNP200*, *SRRM1* and *SRSF3* resulted in a significantly increase of the expression levels of *PTEN* (Fig. 5d).

3.5. Silencing of *SNRNP200*, *SRRM1* and *SRSF3* enhanced the antitumor actions of enzalutamide in PCa cells

In order to test the effects of *SNRNP200*-, *SRRM1*- and *SRSF3*-silencing on androgens and enzalutamide responsiveness, we evaluated proliferation rate of 22Rv1 and LNCaP cells after 24h. We used this experimental paradigm in that cell proliferation was not significantly

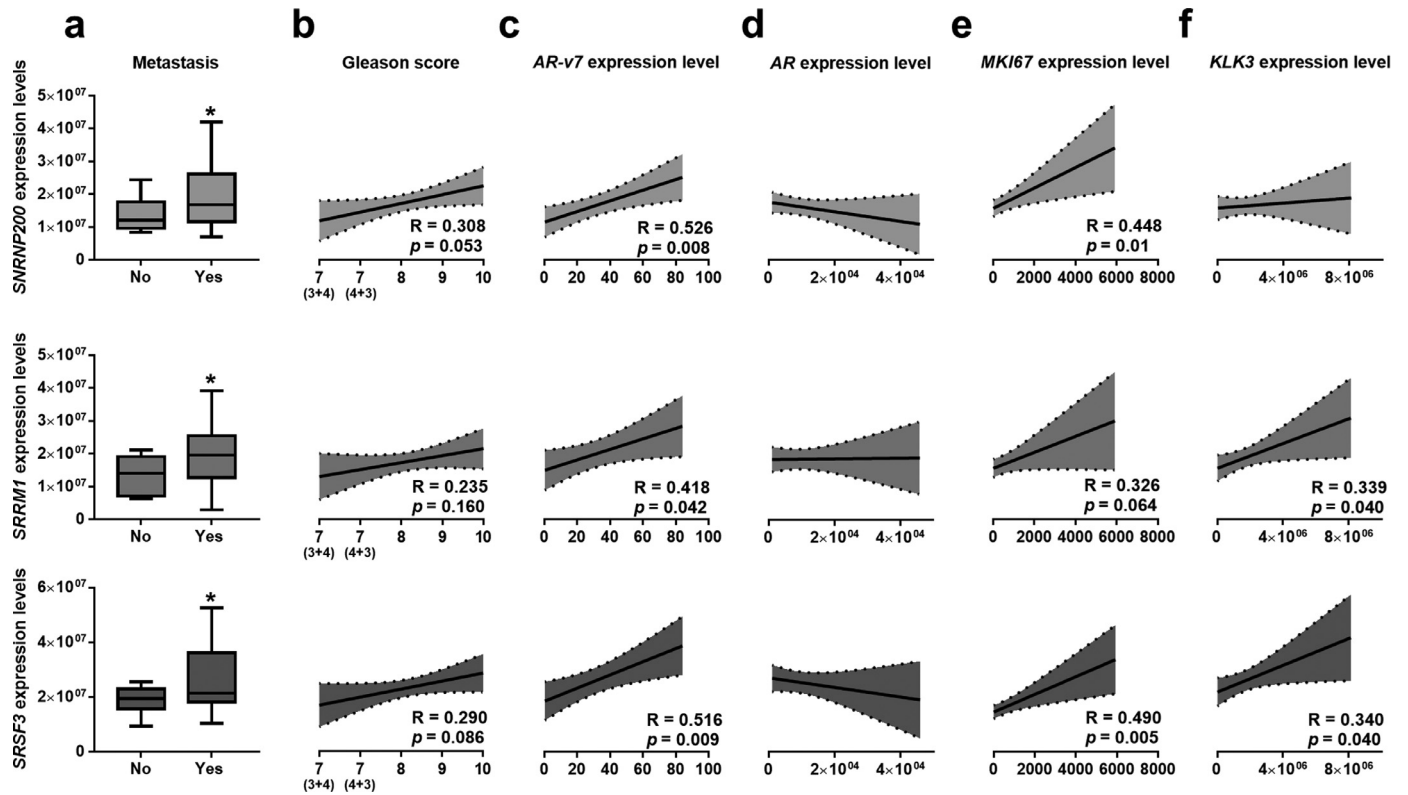


**Fig. 2.** Expression of *SNRNP200*, *SRRM1* and *SRSF3* in a highly aggressive cohort of prostate cancer (PCa) samples. (a) *SNRNP200*, *SRRM1* and *SRSF3* expression levels in a battery of highly-aggressive PCa samples, with or without the presence of metastasis (n = 42). represent the mean ± SEM of mRNA expression levels. b-f) Correlation between *SNRNP200*, *SRRM1* and *SRSF3* expression levels and Gleason score (b), expression levels of *AR-v7* (c), *AR* (d) *MKI67* (e) and *KLK3* (f). mRNA levels were determined by a microfluidic-based qPCR array and adjusted by normalization factor calculated from *ACTB* and *GAPDH* expression levels. Asterisk (\* p < 0.05) indicates statistically significant differences between groups.

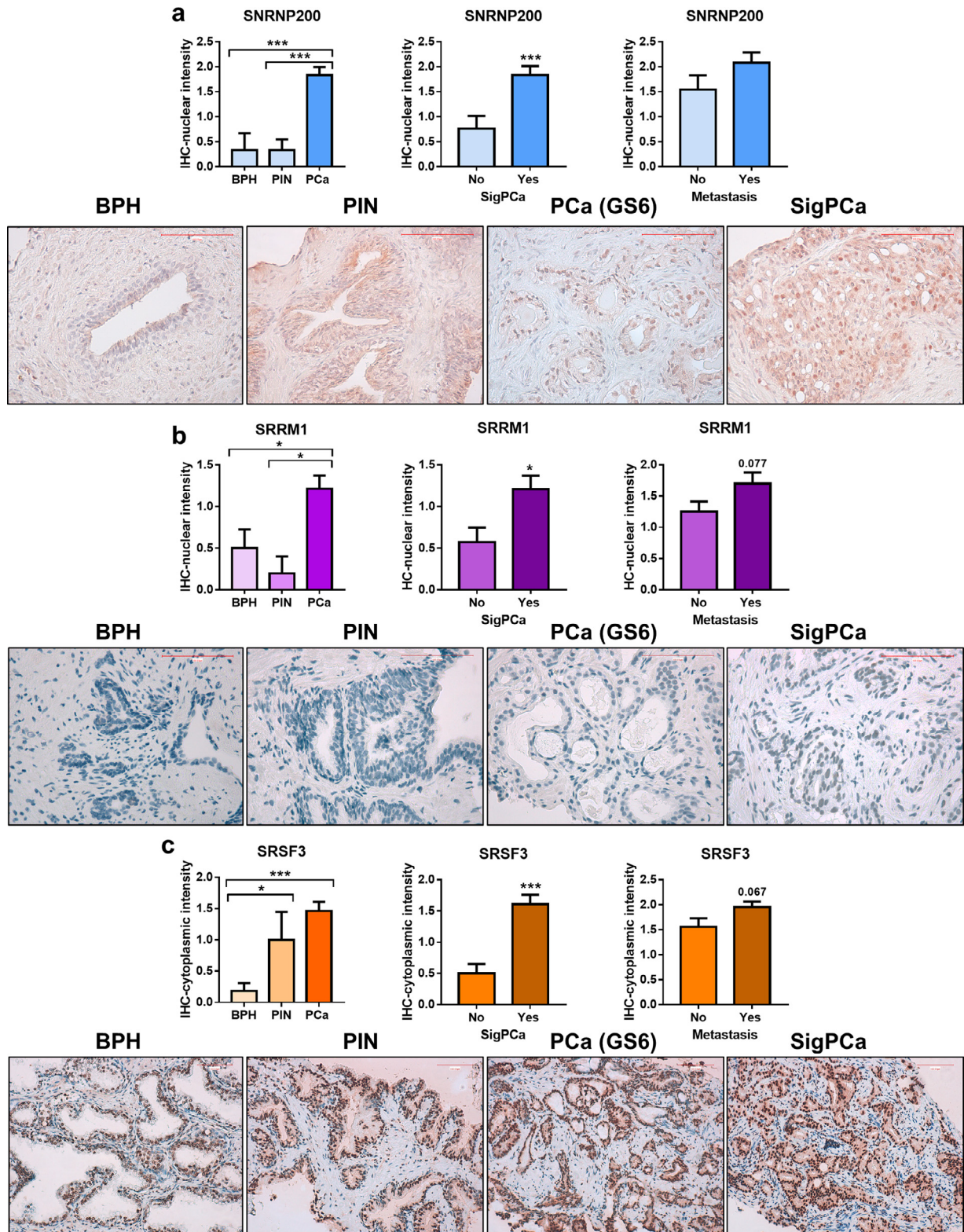


**Fig. 3.** Immunohistochemical analysis of SNRNP200, SRRM1 and SRSF3 in prostate cancer (PCa) samples. a) Comparison of SNRNP200, SRRM1 (b) and SRSF3 (c) protein levels by immunohistochemistry (IHC) between a representative set of PCa samples ( $n = 47$ ), prostatic intraepithelial neoplasia (PIN;  $n = 6$ ) and benign prostatic hyperplasia (BPH;  $n = 7$ ). Association of protein levels with clinically significant PCa (SigPCa; defined as Gleason score higher than 7) and the presence of metastasis at diagnosis (central panel and right panel, respectively). Representative images of BPH, PIN, PCa with Gleason score = 6 and SigPCa stained with SNRNP200 (400 $\times$  magnification), SRRM1 (400 $\times$  magnification) and SRSF3 (200 $\times$  magnification) antibodies are showed below a, b and c panels, respectively. Scale bar indicates 100  $\mu$ m. Data are expressed as mean  $\pm$  SEM of IHC staining scaled from low [1] to high [3] intensity. Asterisks (\*  $p < 0.05$ ; \*\*  $p < 0.01$ ; \*\*\*  $p < 0.001$ ) indicate statistically significant differences between groups.

compromised after 24h of enzalutamide treatment nor by 24h of SNRNP200-, SRRM1- and SRSF3-silencing (Fig. 6a, open bars) in 22Rv1 cells. Firstly, we observed that the silencing of SNRNP200, SRRM1 or

SRSF3 did not alter the normal (scramble-treated) response to DHT as a similar decrease of proliferation rate was found compared to DHT-treated cells, independently of the siRNA used (i.e. scramble,



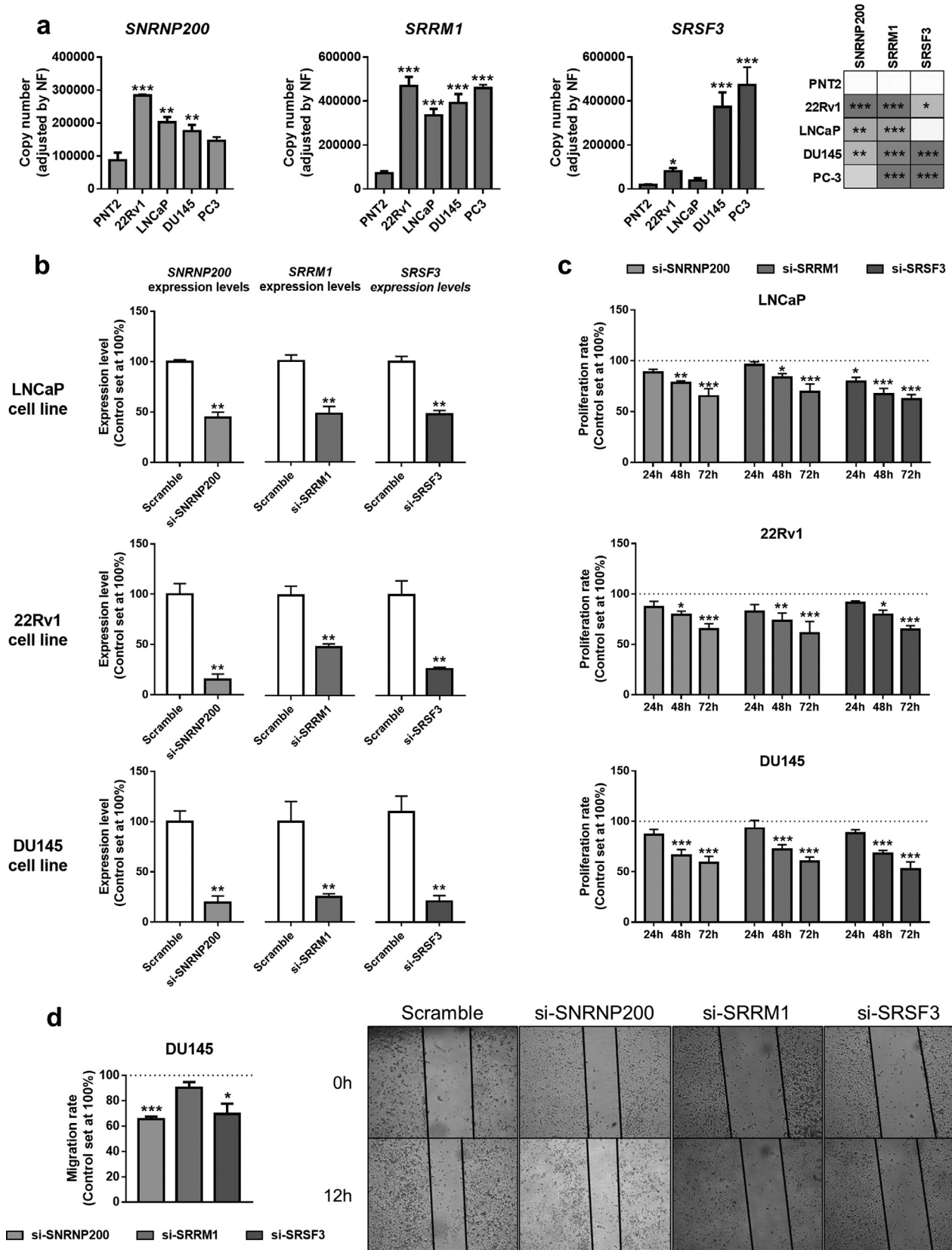


**Fig. 4.** Functional consequences of *SNRNP200*, *SRRM1* and *SRSF3* silencing in prostate-derived cell lines. a) Comparison of *SNRNP200*, *SRRM1* and *SRSF3* expression levels between a non-tumor prostate cell line (PNT2) and Pca cell lines LNCaP, 22Rv1, DU145 and PC-3 ( $n = 5$ ). mRNA levels were determined by qPCR and adjusted by normalization factor calculated from *ACTB* and *GAPDH* expression levels. b) Validation by qPCR of *SNRNP200*, *SRRM1* and *SRSF3* silencing (si-SNRNP200, si-SRRM1 and si-SRSF3, respectively). mRNA levels were determined by qPCR and adjusted by normalization factor calculated from *ACTB* and *GAPDH* expression levels. Data were represented as percent of scramble cells (mean  $\pm$  SEM). c) Proliferation rate of LNCaP (upper panel), 22Rv1 (middlepanel) and DU145 (bottom panel) cell lines after 24-, 48- and 72 h of *SNRNP200*-, *SRRM1*- and *SRSF3*-silencing ( $n = 4$ ). d) Effect of *SNRNP200*-, *SRRM1*- and *SRSF3*-silencing on the migration rate of DU145 cell line was determined by wound-healing assay (12 h;  $n \geq 3$ ). Representative images are depicted in right panel. Data were represented as percent of scramble cells (mean  $\pm$  SEM). Asterisks (\*  $p < 0.05$ ; \*\*  $p < 0.01$ ; \*\*\*  $p < 0.001$ ) indicate statistically significant differences between groups.

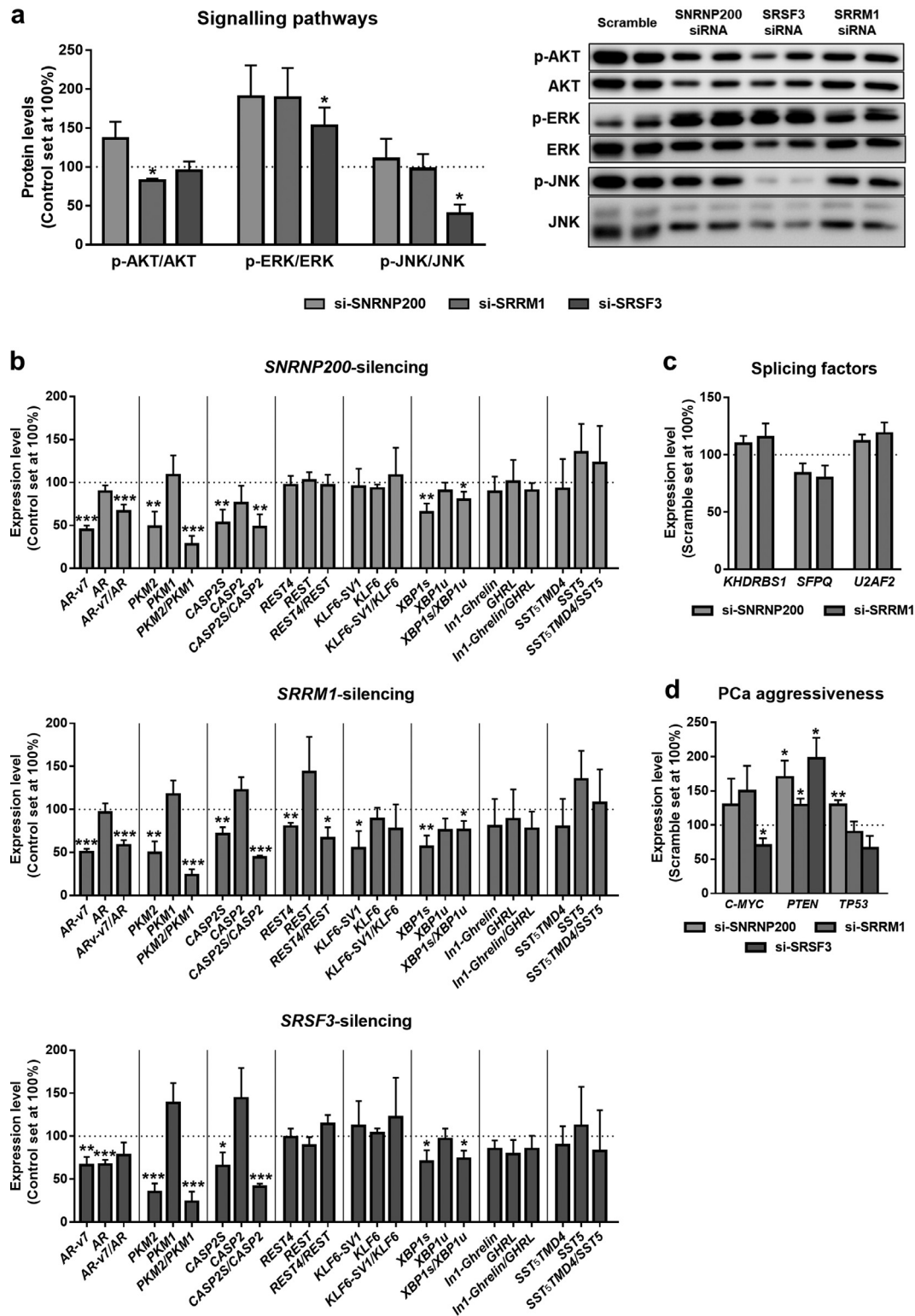


**Fig. 5.** Molecular consequences of *SNRNP200*, *SRRM1* and *SRSF3* silencing in 22Rv1 cell line. a) Basal phospho-AKT, phospho-ERK1/2 and phospho-JNK levels in *SNRNP200*-, *SRRM1*- and *SRSF3* silenced 22Rv1 cells (si-*SNRNP200*, si-*SRRM1* and si-*SRSF3*, respectively; 24 h;  $n \geq 3$ ). Protein levels were normalized by total AKT, ERK and JNK protein levels. Representative images are shown in right panel. Protein data were represented as percent of scramble cells. b) Expression levels of selected transcripts in response to *SNRNP200* (upper panel), *SRRM1* (central panel) and *SRSF3* (bottom panel) silencing (24 h) in 22Rv1 cells. Ratio between the expression of splicing variants is shown in bars with dotted pattern. c) Expression levels of *KHDRBS1*, *SFPQ* and *U2AF2* in response to *SNRNP200*- and *SRRM1*-silencing in 22Rv1 cells. d) Expression levels of *C-MYC*, *PTEN* and *TP53* in response to *SNRNP200*-, *SRRM1*- and *SRSF3*-silencing in 22Rv1 cells. mRNA levels were determined by qPCR and adjusted by normalization factor calculated from *ACTB* and *GAPDH* expression levels. Data were represented as percent of scramble-treated control cells (mean  $\pm$  SEM). Asterisks (\*  $p < 0.05$ ; \*\*  $p < 0.01$ ; \*\*\*  $p < 0.001$ ) indicate statistically significant differences between groups.

si-*SNRNP200*, si-*SRRM1* or si-*SRSF3*) in 22Rv1 and LNCaP cell lines (Fig. 6a/b). However, the silencing of *SNRNP200*, *SRRM1* and *SRSF3* combined with enzalutamide treatment resulted in an additive, statistically

significant antiproliferative effect in 22Rv1 cells at 24h of incubation, indicating that silencing of *SNRNP200*, *SRRM1* or *SRSF3* sensitized 22Rv1 cells to enzalutamide (Fig. 6a). Additionally, although no differences

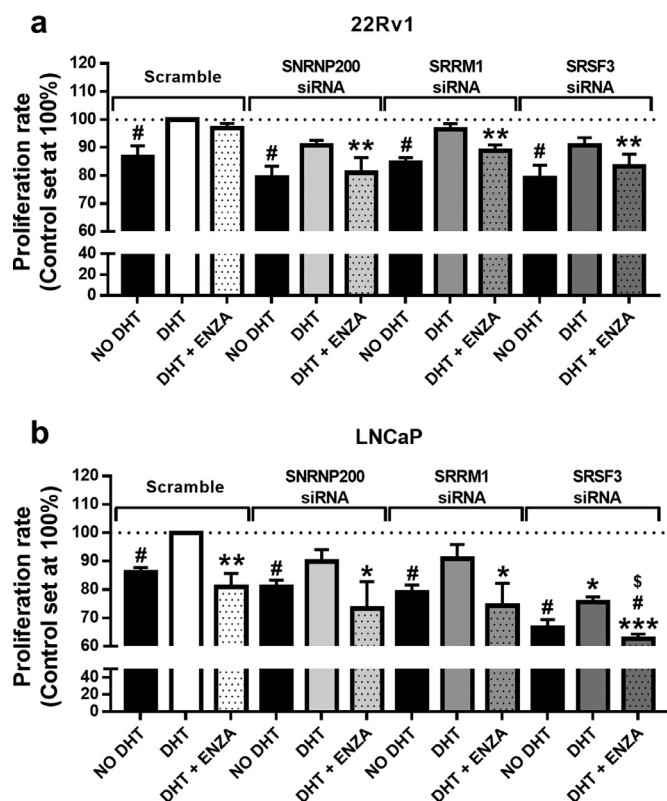


**Fig. 6.** Cell proliferation assay in response to enzalutamide treatment combined with *SNRNP200*, *SRRM1* and *SRSF3* silencing. Proliferation rate of 22Rv1 (a) and LNCaP (b) cell line was measured after 24 h of *SNRNP200*-, *SRRM1*- and *SRSF3*-silencing in the presence (DHT) or absence (no DHT) of  $5\alpha$ -dihydrotestosterone with or without enzalutamide (ENZA;  $n=4$ ). Results were expressed as percentage referred to scramble vehicle-treated control with DHT (mean  $\pm$  SEM). Asterisks (\*  $p < 0.05$ ; \*\*  $p < 0.01$ ), dash (#  $p < 0.05$ ) and dollar sign (\$) ( $p < 0.05$ ) indicate statistically significant differences compared to DHT of scramble, DHT of each condition and DHT+ENZA of scramble, respectively.

were observed when analysing 22Rv1 scramble-treated cells in response to enzalutamide at 24h, we found a significantly decrease in the proliferation rate of scramble-treated LNCaP cells in response to enzalutamide (Fig. 6a/b). Interestingly, the pattern of response of *SNRNP200*- and *SRRM1*-silenced LNCaP cells was similar to scramble-treated LNCaP cells (Fig. 6b), wherein the response to non-DHT and to enzalutamide was comparable in scramble-, si-*SNRNP200*- and si-*SRRM1*-treated LNCaP cells. In striking contrast, the response of *SRSF3*-silenced cells was markedly different. Specifically, the proliferation rate of *SRSF3*-silenced LNCaP cells in the presence of DHT was significantly lower compared to scramble-treated LNCaP cells in the presence of DHT. In addition, we observed that enzalutamide treatment and *SRSF3*-silencing exerted an additive antiproliferative effect in LNCaP cells, inasmuch as the proliferation rate of enzalutamide-treated *SRSF3*-silenced LNCaP cells was significantly lower than that of enzalutamide-treated scramble-treated cells (in presence of DHT) and than that of *SRSF3*-silenced cells (in presence of DHT) (Fig. 6b).

#### 4. Discussion

PCa is one of the tumor pathologies whose development and, specially, progression is mostly influenced by the alteration of the normal gene expression pattern and the aberrant presence of oncogenic SVs [24]. Indeed, PCa is drastically influenced by the appearance of the AR splicing variant-7 (AR-v7), inasmuch as it has been strongly associated with PCa aggressiveness [25], as well as with the resistance to conventional therapies such as antiandrogens and chemotherapy [26,27]. Similarly, the altered expression pattern of additional SVs, such as *SST5TMD4*

[4], *PKM2* [5], *REST4* [6], *XBP1s* [7], *In1-Ghrelin* [8] among others, has also been found to be associated to PCa development and progression. In this sense, it is reasonable to think that a dysregulation of the cellular machinery involved in the control of splicing process would be responsible for the broad alteration of oncogenic SVs observed in PCa. However, although some specific SFs and SCs have been associated with PCa development and aggressiveness [22,23,28–30], to the best of our knowledge, no studies have comprehensively explored the global dysregulations of these elements in PCa.

In our study, we have demonstrated for the first time a profound and overt dysregulation of the expression levels of a representative set of SCs and associated SFs in PCa. In particular, more than 50% of the SCs and SFs analysed herein displayed an altered expression pattern, demonstrating that the components of the cellular machinery responsible for the processing of the splicing process are drastically dysregulated in PCa. Indeed, we have bioinformatically defined an expression-based molecular fingerprint (combining the mRNA expression levels of 11 SCs and SFs) able to perfectly discriminate between PCa and non-tumor adjacent regions, which further reinforces this contention and demonstrate that PCa curses with a global dysregulation of the splicing machinery. Even more important is the fact that the expression levels of many of the SCs and SFs determined in this study were associated or correlated with relevant clinical and molecular features of aggressiveness (e.g. Gleason score, presence of metastasis and *AR-v7* expression), suggesting a causal link between the dysregulations of the splicing machinery and the aggressiveness of PCa. These results are consistent with and further expand previous observations indicating that high expression of specific SFs, including *RBM3*, *U2AF2*, *ESRP1*, *ESRP2* and *NOVA1* among others, is associated to clinical and/or molecular PCa aggressiveness features [23,28,30,31].

Among all the SCs and SFs analysed herein, *SNRNP200*, *SRRM1* and *SRSF3* seemed to have special relevance in PCa pathophysiology in that their expression levels were significantly up-regulated and associated with all the relevant clinical features analysed in this study, including Gleason score, pathological stage, perineural invasion, lymphovascular invasion, biochemical recurrence, presence of metastasis at diagnosis or *AR-v7* expression. Importantly, data available *in silico* further validated the overexpression of *SNRNP200*, *SRRM1* and *SRSF3* in PCa as compared to non-tumoral prostate tissues [i.e. Singh, Wallace, Tomlins and/or Welsh-dataset [32–35]]. In addition, these splicing machinery components could represent novel biomarkers and/or therapeutic targets in PCa inasmuch as their dysregulation has not been previously described in this tumor pathology and their expression levels showed a potential utility as prognostic markers, since these levels were associated with biochemical recurrence. It should be noted that, although *SRSF3* has been defined as an oncogene in different tumor pathologies [36–38], this is the first description of the overexpression of this SF in PCa. Specifically, it has been shown that *SRSF3* can enhance aggressiveness features of several tumor types through the control of splicing process in the nucleus [37,39,40], but also through the alteration of translational efficiency of certain mRNAs in the cytoplasm [41]. This suggests that overexpression of *SRSF3* mRNA can exert oncogenic actions either by increasing *SRSF3* protein levels in the nucleus or in the cytoplasm, as found herein in the case of PCa cells. On the other hand, the protein overexpression of *SRRM1* and *SNRNP200* was observed in the nucleus of PCa cells, suggesting an enhancement of their putative activity as splicing modulators in these cells.

Due to the increasing body of evidence pointing toward a strong dysregulation of the splicing process in cancer, many therapeutic strategies to prevent the expression of oncogenic SVs and/or to modulate the activity of the spliceosome have been reported hitherto [42]. In particular, during the last years, many spliceosome inhibitors (e.g. Pladienolide-B, spliceostatin-A) have been reported and suggested as therapeutic targets in different pathologies wherein the dysregulated splicing process has been shown to be relevant [43,44].

However, while blocking the activity of the spliceosome could be less specific, targeting specific SCs and/or SFs could represent a novel and more specific approach to tackle cancer diseases in that a more reduced number but better-defined splicing events may be altered. In this sense, we have demonstrated for the first time herein that the silencing of the expression of *SNRNP200*, *SRRM1* and *SRSF3* using specific siRNAs clearly decreased key functional parameters of aggressiveness, including proliferation and migration, in PCa-derived cell lines. These clinically relevant antitumor actions seemed to be associated to the modulation of key signaling pathways and the expression of certain oncogenic SVs. Indeed, *SRRM1*- and *SRSF3*-silencing evoked a decrease in phosphorylation levels of AKT and JNK proteins, respectively, probably leading to the inhibition of PI3K/AKT and JNK pathways, which have been broadly defined as oncogenic signaling pathways [45,46]. Intriguingly, the silencing of *SRSF3* increased ERK-phosphorylation, presumably leading to a higher activation of MAPK/ERK pathway, which has been reported to be highly susceptible to be dysregulated in response to splicing changes [47]. Remarkably, despite its well-known oncogenic role, MAPK/ERK-pathway has been postulated as a regulator of cell senescence, thus also exerting antitumor effects [48]. As expected, and providing a mechanistic explanation, *SNRNP200*-, *SRRM1*- and *SRSF3*-silencing dysregulated the splicing process of several genes involved in tumor aggressiveness, such as *AR*, *PKM*, *CASP2* or *XBP1*. Among them, especially relevant are the results obtained in *AR* splicing, due to its well-known role in the development and aggressiveness of PCa [49]. Specifically, a decrease in the expression of *AR-v7* (but not *AR*) was observed in response to *SNRNP200*- and *SRRM1*-silencing, thus altering the normal splicing process of *AR*. Interestingly, the modulation of *AR* splicing process exerted by *SNRNP200* and *SRRM1* may be not mediated by the regulation of splicing factors previously reported to be involved in *AR-v7* generation such as *KHDRBS1* [21], *SFPQ* [22] or *U2AF2* [23], inasmuch as we found that the silencing of *SNRNP200* and *SRRM1* did not alter the expression levels of these *AR*-splicing modulators. On the other hand, the silencing of *SRSF3* decreased the expression levels of both *AR* and *AR-v7*. In any case, these results postulate these three factors as potential therapeutic target candidates to tackle castration resistant PCa (CRPC), since *AR-v7* has been reported as a driver of CRPC-development [50]. Reinforcing the oncogenic role of *SNRNP200*, *SRRM1* and *SRSF3* in PCa, we found that the silencing of these genes resulted in the modulation of the expression of key genes involved in CRPC aggressiveness, including *C-MYC*, *PTEN* and/or *TP53* [51–53]. Consistently, *SNRNP200*-, *SRRM1*- and *SRSF3*-silencing sensitized 22Rv1 cells to enzalutamide by showing additive effects in the inhibition of proliferation rate in these cells, possibly through *AR-v7* down-regulation. This hypothesis was reinforced by the fact that *SNRNP200*- or *SRRM1*-silencing did not alter the normal response to enzalutamide in LNCaP cell line (which express *AR* but lack *AR-v7*), while *SRSF3*-silencing (which is associated to a reduction in full-length *AR* expression) in combination with enzalutamide treatment resulted in an additive antiproliferative effect in these cells.

Therefore, the data presented herein indicate that the cellular machinery responsible for the regulation of the splicing process is drastically altered in PCa and that certain SCs and SVs could represent novel candidates as potential diagnostic and prognostic biomarkers, as well as putative targets to develop novel therapeutic strategies against PCa. Specifically, our results demonstrated that *SNRNP200*, *SRRM1* and *SRSF3* could represent attractive novel diagnostic/prognostic and therapeutic targets for PCa and CRPC.

## 5. Role of the funding sources

This work was funded by Instituto de Salud Carlos III, co-funded by European Union (ERDF/ESF, “Investing in your future”) [PI16/00264, PI17-02287, CM16/00180, FI17/00282, CD16/00092], FEDER (CCB.030PM), MINECO/MECD (BFU2016-80360-R; FPU16/06190,

FPU18/02485, FPU16/05059, FPU17/00263, FPU14/04290), Junta de Andalucía (BIO-0139), Spanish Association Against Cancer (AECC; INVES18057YUBE) and CIBERobn. CIBER is an initiative of Instituto de Salud Carlos III, Ministerio de Sanidad, Servicios Sociales e Igualdad, Spain. The biological samples repository node (Córdoba, Spain) is gratefully acknowledged for coordination tasks in the selection of samples.

All the funding sources were essential for data collection, analysis, interpretation and patient recruitment. The corresponding author declare that he had full access to all the data in the study and had the final responsibility for the decision to submit for publication.

## Author's contributions

*Juan Manuel Jiménez-Vacas*: Conceptualization, Data curation, Formal analysis, Investigation, Methodology, Validation, Visualization, Writing - original draft, Writing - review & editing. *Vicente Herrero-Aguayo, Antonio Jesús Montero-Hidalgo*: Conceptualization, Data curation, Formal analysis, Investigation, Methodology, Validation, Visualization, Writing - review & editing. *Enrique Gómez-Gómez*: Conceptualization, Data curation, Formal analysis, Investigation, Methodology, Validation, Resources, Writing - review & editing. *Antonio C. Fuentes-Fayos, Antonio José León-González, Prudencio Sáez-Martínez, Emilia Alors-Pérez, Sergio Pedraza-Arévalo, Teresa González-Serrano, Oscar Reyes, Ana Martínez-López, Rafael Sánchez-Sánchez and Elena M Yubero-Serrano*: Data curation, Formal analysis, Investigation, Writing - review and editing. *Sebastián Ventura*: Data curation, Formal analysis, Investigation, Software, Writing - review and editing. *María J. Requena-Tapia, Justo P. Castaño and Manuel D. Gahete*: Formal analysis, Methodology, Resources, Writing - original draft, Writing - review & editing. *Raúl M. Luque*: Conceptualization, Data curation, Formal analysis, Funding acquisition, Investigation, Methodology, Project administration, Resources, Supervision, Visualization, Writing - original draft, Writing - review & editing.

## Declaration of Competing Interest

The authors declare that they have no conflict of interest.

## Supplementary materials

Supplementary material associated with this article can be found in the online version at doi:10.1016/j.ebiom.2019.11.008.

## References

- [1] Matera AG, Wang Z. A day in the life of the spliceosome. *Nat Rev Mol Cell Biol* 2014;15(2):108–21.
- [2] Scotti MM, Swanson MS. RNA mis-splicing in disease. *Nat Rev Genet* 2016;17(1):19–32.
- [3] Bray F, Ferlay J, Soerjomataram I, Siegel RL, Torre LA, Jemal A. Global cancer statistics 2018: GLOBOCAN estimates of incidence and mortality worldwide for 36 cancers in 185 countries. *CA Cancer J Clin* 2018;68(6):394–424.
- [4] Hormaechea-Agulla D, Jimenez-Vacas JM, Gomez-Gomez E, F LL, Carrasco-Valiente J, Valero-Rosa J, et al. The oncogenic role of the spliced somatostatin receptor st5TMD4 variant in prostate cancer. *Faseb J* 2017;31(11):4682–96.
- [5] Wong N, Yan J, Ojo D, De Melo J, Cutz JC, Tang D. Changes in PKM2 associate with prostate cancer progression. *Cancer Invest* 2014;32(7):330–8.
- [6] Zhang X, Coleman IM, Brown LG, True LD, Kollath L, Lucas JM, et al. *SRRM4* expression and the loss of rest activity may promote the emergence of the neuroendocrine phenotype in castration-resistant prostate cancer. *Clin Cancer Res* 2015;21(20):4698–708.
- [7] Sheng X, Nenseth HZ, Qu S, Kuzu OF, Frahnaw T, Simon L, et al. *IRE1α-XBP1s* pathway promotes prostate cancer by activating c-MYC signaling. *Nat Commun* 2019;10(1):323.
- [8] Hormaechea-Agulla D, Gahete MD, Jimenez-Vacas JM, Gomez-Gomez E, Ibanez-Costa A, F LL, et al. The oncogenic role of the In1-ghrelin splicing variant in prostate cancer aggressiveness. *Mol Cancer* 2017;16(1):146.
- [9] Zhang C, Li HR, Fan JB, Wang-Rodriguez J, Downs T, Fu XD, et al. Profiling alternatively spliced mRNA isoforms for prostate cancer classification. *BMC Bioinform* 2006;7:202.

- [10] Pedraza-Arevalo S, Hormaechea-Agulla D, Gomez-Gomez E, Requena MJ, Selth LA, Gahete MD, et al. Somatostatin receptor subtype 1 as a potential diagnostic marker and therapeutic target in prostate cancer. *Prostate* 2017;77(15):1499–511.
- [11] Del Rio-Moreno M, Alors-Perez E, Gonzalez-Rubio S, Ferrin G, Reyes O, Rodriguez-Peralvarez M, et al. Dysregulation of the splicing machinery is associated to the development of non-alcoholic fatty liver disease. *J Clin Endocrinol Metab* 2019.
- [12] Gahete MD, Del Rio-Moreno M, Camargo A, Alcalá-Díaz JF, Alors-Perez E, Delgado-Lista J, et al. Changes in splicing machinery components influence, precede, and early predict the development of type 2 diabetes: from the cordioprev study. *EBioMedicine* 2018;37:356–65.
- [13] Vandesompele J, De Preter K, Pattyn F, Poppe B, Van Roy N, De Paep A, et al. Accurate normalization of real-time quantitative rt-pcr data by geometric averaging of multiple internal control genes. *Genome Biol* 2002;3(7) research0034.1.
- [14] Luque RM, Ibanez-Costa A, Neto LV, Taboada GF, Hormaechea-Agulla D, Kasuki L, et al. Truncated somatostatin receptor variant sst5TMD4 confers aggressive features (proliferation, invasion and reduced octreotide response) to somatotropinomas. *Cancer Lett* 2015;359(2):299–306.
- [15] Ibanez-Costa A, Gahete MD, Rivero-Cortes E, Rincon-Fernandez D, Nelson R, Beltran M, et al. In1-ghrelin splicing variant is overexpressed in pituitary adenomas and increases their aggressive features. *Sci Rep* 2015;5:8714.
- [16] Duran-Prado M, Gahete MD, Hergueta-Redondo M, Martinez-Fuentes AJ, Cordoba-Chacon J, Palacios J, et al. The new truncated somatostatin receptor variant sst5TMD4 is associated to poor prognosis in breast cancer and increases malignancy in MCF-7 cells. *Oncogene* 2012;31(16):2049–61.
- [17] Sampedro-Nunez M, Luque RM, Ramos-Levi AM, Gahete MD, Serrano-Somavilla A, Villa-Osaba A, et al. Presence of sst5TMD4, a truncated splice variant of the somatostatin receptor subtype 5, is associated to features of increased aggressiveness in pancreatic neuroendocrine tumors. *Oncotarget* 2016;7(6):6593–608.
- [18] Hatami R, Sieuwerts AM, Izadmehr S, Yao Z, Qiao RF, Papa L, et al. KLF6-SV1 drives breast cancer metastasis and is associated with poor survival. *Sci Transl Med* 2013;5(169) 169ra12.
- [19] Kuranagan Y, Sugito N, Shinohara H, Tsujino T, Taniguchi K, Komura K, et al. SRSF3, a splicer of the PKM gene, regulates cell growth and maintenance of cancer-specific energy metabolism in colon cancer cells. *Int J Molecular Sci* 2018;19(10).
- [20] Li Y, Donmez N, Sahinalp C, Xie N, Wang Y, Xue H, et al. SRRM4 drives neuroendocrine transdifferentiation of prostate adenocarcinoma under androgen receptor pathway inhibition. *Eur Urol* 2017;71(1):68–78.
- [21] Stockley J, Markert E, Zhou Y, Robson CN, Elliott DJ, Lindberg J, et al. The RNA-binding protein Sam68 regulates expression and transcription function of the androgen receptor splice variant AR-V7. *Sci Rep* 2015;5:13426.
- [22] Takayama KI, Suzuki T, Fujimura T, Yamada Y, Takahashi S, Homma Y, et al. Dysregulation of spliceosome gene expression in advanced prostate cancer by RNA-binding protein PSF. *PNAS* 2017;114(39):10461–6.
- [23] Liu LL, Xie N, Sun S, Plymate S, Mostaghel E, Dong X. Mechanisms of the androgen receptor splicing in prostate cancer cells. *Oncogene* 2014;33(24):3140–50.
- [24] Paschalis A, Sharp A, Welti JC, Neeb A, Raj GV, Luo J, et al. Alternative splicing in prostate cancer. *Nat Rev Clin Oncol* 2018;15(11):663–75.
- [25] Kong D, Sethi S, Li Y, Chen W, Sakr WA, Heath E, et al. Androgen receptor splice variants contribute to prostate cancer aggressiveness through induction of EMT and expression of stem cell marker genes. *Prostate* 2015;75(2):161–74.
- [26] Antonarakis ES, Lu C, Wang H, Lubner B, Nakazawa M, Roeser JC, et al. AR-V7 and resistance to enzalutamide and abiraterone in prostate cancer. *N Engl J Med* 2014;371(11):1028–38.
- [27] Antonarakis ES, Lu C, Lubner B, Wang H, Chen Y, Nakazawa M, et al. Androgen receptor splice variant 7 and efficacy of taxane chemotherapy in patients with metastatic castration-resistant prostate cancer. *JAMA Oncol* 2015;1(5):582–91.
- [28] Grupp K, Wilking J, Prien K, Hube-Magg C, Sirma H, Simon R, et al. High RNA-binding motif protein 3 expression is an independent prognostic marker in operated prostate cancer and tightly linked to ERG activation and PTEN deletions. *Eur J Cancer* 2014;50(4):852–61.
- [29] Yamamoto R, Osawa T, Sasaki Y, Yamamoto S, Anai M, Izumi K, et al. Overexpression of p54(nrb)/NONO induces differential EPHA6 splicing and contributes to castration-resistant prostate cancer growth. *Oncotarget* 2018;9(12):10510–24.
- [30] Gerhauser C, Favero F, Risch T, Simon R, Feuerbach L, Assenov Y, et al. Molecular evolution of early-onset prostate cancer identifies molecular risk markers and clinical trajectories. *Cancer Cell* 2018;34(6) 996–1011.e8.
- [31] Lu ZX, Huang Q, Park JW, Shen S, Lin L, Tokheim CJ, et al. Transcriptome-wide landscape of pre-mRNA alternative splicing associated with metastatic colonization. *Mol Cancer Res* 2015;13(2):305–18.
- [32] Singh D, Febbo PG, Ross K, Jackson DG, Manola J, Ladd C, et al. Gene expression correlates of clinical prostate cancer behavior. *Cancer Cell* 2002;1(2):203–9.
- [33] Wallace TA, Prueitt RL, Yi M, Howe TM, Gillespie JW, Yfantis HG, et al. Tumor immunobiological differences in prostate cancer between African-American and European-American men. *Cancer Res* 2008;68(3):927–36.
- [34] Kim JH, Dhanasekaran SM, Mehra R, Tomlins SA, Gu W, Yu J, et al. Integrative analysis of genomic aberrations associated with prostate cancer progression. *Cancer Res* 2007;67(17):8229–39.
- [35] Welsh JB, Sapinoso LM, Su AI, Kern SG, Wang-Rodriguez J, Moskaluk CA, et al. Analysis of gene expression identifies candidate markers and pharmacological targets in prostate cancer. *Cancer Res* 2001;61(16):5974–8.
- [36] Peiqi L, Zhaozhong G, Yaotian Y, Jun J, Jihua G, Rong J. Expression of SRSF3 is correlated with carcinogenesis and progression of oral squamous cell carcinoma. *Int J Med Sci* 2016;13(7):533–9.
- [37] Gautrey H, Jackson C, Ditttrich AL, Browell D, Lennard T, Tyson-Capper A. SRSF3 and hnRNP H1 regulate a splicing hotspot of HER2 in breast cancer cells. *RNA Biol* 2015;12(10):1139–51.
- [38] Lin JC, Lee YC, Tan TH, Liang YC, Chuang HC, Fann YC, et al. RBM4-SRSF3-MAP4K4 splicing cascade modulates the metastatic signature of colorectal cancer cell. *Biochimica et Biophysica Acta Molecular Cell Res* 2018;1865(2):259–72.
- [39] Wang H, Zhang CZ, Lu SX, Zhang MF, Liu LL, Luo RZ, et al. A coiled-coil domain containing 50 splice variant is modulated by serine/arginine-rich splicing factor 3 and promotes hepatocellular carcinoma in mice by the ras signaling pathway. *Hepatology (Baltimore, Md)* 2019;69(1):179–95.
- [40] Zhu S, Chen Z, Katsha A, Hong J, Belkhir A, El-Rifai W. Regulation of CD44E by DARPP-32-dependent activation of Srp20 splicing factor in gastric tumorigenesis. *Oncogene* 2016;35(14):1847–56.
- [41] Kim J, Park RY, Chen JK, Kim J, Jeong S, Ohn T. Splicing factor SRSF3 represses the translation of programmed cell death 4 mRNA by associating with the 5'-UTR region. *Cell Death Differ* 2014;21(3):481–90.
- [42] Jyotsana N, Heuser M. Exploiting differential RNA splicing patterns: a potential new group of therapeutic targets in cancer. *Expert Opin Ther Targets* 2018;22(2):107–21.
- [43] Sato M, Muguruma N, Nakagawa T, Okamoto K, Kimura T, Kitamura S, et al. High antitumor activity of pladienolide B and its derivative in gastric cancer. *Cancer Sci* 2014;105(1):110–6.
- [44] Larrayoz M, Blakemore SJ, Dobson RC, Blunt MD, Rose-Zerilli MJ, Walewska R, et al. The SF3B1 inhibitor spliceostatin A (SSA) elicits apoptosis in chronic lymphocytic leukaemia cells through downregulation of Mcl-1. *Leukemia* 2016;30(2):351–60.
- [45] Chen H, Zhou L, Wu X, Li R, Wen J, Sha J, et al. The PI3K/AKT pathway in the pathogenesis of prostate cancer. *Front Biosci (Landmark Ed)* 2016;21:1084–91.
- [46] Hubner A, Mulholland DJ, Standen CL, Karasrides M, Cavanagh-Kyros J, Barrett T, et al. JNK and pten cooperatively control the development of invasive adenocarcinoma of the prostate. *PNAS* 2012;109(30):12046–51.
- [47] Siegfried Z, Bonomi S, Ghigna C, Karni R. Regulation of the Ras-MAPK and PI3K-mTOR signalling pathways by alternative splicing in cancer. *Int J Cell Biol* 2013;2013:568931.
- [48] Deschenes-Simard X, Gaumont-Leclerc MF, Bourdeau V, Lessard F, Moiseeva O, Forest V, et al. Tumor suppressor activity of the erk/mapk pathway by promoting selective protein degradation. *Genes Dev* 2013;27(8):900–15.
- [49] Tan MH, Li J, Xu HE, Melcher K, Yong EL. Androgen receptor: structure, role in prostate cancer and drug discovery. *Acta Pharmacol Sin* 2015;36(1):3–23.
- [50] Qu Y, Dai B, Ye D, Kong Y, Chang K, Jia Z, et al. Constitutively active AR-V7 plays an essential role in the development and progression of castration-resistant prostate cancer. *Sci Rep* 2015;5:7654.
- [51] Bai S, Cao S, Jin L, Kobelski M, Schouest B, Wang X, et al. A positive role of c-Myc in regulating androgen receptor and its splice variants in prostate cancer. *Oncogene* 2019;38(25):4977–89.
- [52] Jamaspishvili T, Berman DM, Ross AE, Scher HI, De Marzo AM, Squire JA, et al. Clinical implications of PTEN loss in prostate cancer. *Nat Rev Urol* 2018;15(4):222–34.
- [53] Hamid AA, Gray KP, Shaw G, MacConaill LE, Evan C, Bernard B, et al. Compound genomic alterations of TP53, PTEN, and RB1 tumor suppressors in localized and metastatic prostate cancer. *Eur Urol* 2019;76(1):89–97.